

Pseudogap and the specific heat of high T_c superconductors

E. J. Calegari*

Laboratório de Teoria da Matéria Condensada,
Departamento de Física - UFSM, 97105-900, Santa Maria, RS, Brazil

S. G. Magalhaes

Instituto de Física, Universidade Federal Fluminense
Av. Litorânea s/n, 24210, 346, Niterói, Rio de Janeiro, Brazil

C. M. Chaves and A. Troper

Centro Brasileiro de Pesquisas Físicas
Rua Xavier Sigaud 150, 22290-180, Rio de Janeiro, RJ, Brazil

August 9, 2018

Abstract

The specific heat of a two dimensional repulsive Hubbard model with local interaction is investigated. We use the two-pole approximation which exhibits explicitly important correlations that are sources of the pseudogap anomaly. The interplay between the specific heat and the pseudogap is the main focus of the present work. Our self consistent numerical results show that above the occupation $n_T \approx 0.85$, the specific heat starts to decrease due to the presence of a pseudogap in the density of states. We have also observed a two peak structure in the specific heat. Such structure is robust with respect to the Coulomb interaction U but it is significantly affected by the occupation n_T . A detailed study of the two peak structure is carried out in terms of the renormalized quasi-particle bands. The role of the second nearest neighbor hopping on the specific heat behavior and on the pseudogap, is extensively discussed.

1 Introduction

The one-band Hubbard model with repulsive local interaction [1] is one of the simplest but sig-

nificant lattice models which allows to describe a rich phenomenology of strong correlated electron systems. Such model has become even more important after the discovery of the high temperature superconductors (HTSC) [2]. Nevertheless, although the two dimensional one-band Hubbard model has been intensively investigated within different levels of approximation, there are still open issues, for instance, the existence of superconductivity and pseudogap [3, 4, 5].

The nature of the pseudogap is one important key to understanding HTSC. A substantial indication of pseudogap can be confirmed through the analysis of the specific heat behavior [6, 7]. From the theoretical point of view, different approaches [8, 9, 10] have been used to investigate the specific heat of the one-band Hubbard model. However, the focus has been on the observed two peak structure rather than its connection with the pseudogap. Monte Carlo simulation [11] and dynamical mean field approximation [12] on the two dimensional one-band Hubbard Model showed evidences of a pseudogap. But such calculations were carried out only at half filling.

In this work, we calculate the electronic specific heat out of the half-filling ($n_T < 1$, where $n_T = n_\sigma + n_{-\sigma}$) for the local repulsive Hubbard model. The Green's functions have been obtained

*eleonir@ufsm.br

in a two-pole approximation [13, 14] which takes into account essential correlations that allow to capture important properties of the pseudogap. In addition to the nearest neighbor hopping, the Hubbard model considered in the present work includes hopping to second nearest neighbors. Such hopping enhances the spin-spin correlations that affect both the pseudogap and the specific heat structure. We present results for the normal phase, i. e., $T > T_c$ where T_c is the superconducting critical temperature. Firstly, the two peak structure of the specific heat is analyzed in terms of the renormalized quasiparticle band. Then, the pseudogap and its interplay with the specific heat, is discussed.

2 Model and general formulation

The model investigated is the two-dimensional one-band Hubbard model [1]

$$H = \sum_{\langle\langle ij \rangle\rangle\sigma} t_{ij} d_{i\sigma}^\dagger d_{j\sigma} + \frac{U}{2} \sum_{i\sigma} n_{i,\sigma} n_{i,-\sigma} - \mu \sum_{i\sigma} n_{i\sigma} \quad (1)$$

where $d_{i\sigma}^\dagger$ ($d_{i\sigma}$) is the fermionic creation (annihilation) operator at site i with spin $\sigma = \{\uparrow, \downarrow\}$ and $n_{i,\sigma} = d_{i\sigma}^\dagger d_{i\sigma}$ is the number operator. The quantity t_{ij} represents the hopping between sites i and j and $\langle\langle \dots \rangle\rangle$ indicates the sum over the first and second-nearest-neighbors of i and μ is the chemical potential. U is the repulsive Coulomb potential between the d electrons localized at the same site i . The bare dispersion relation is

$$\varepsilon_{\vec{k}} = 2t[\cos(k_x a) + \cos(k_y a)] + 4t_2 \cos(k_x a) \cos(k_y a) \quad (2)$$

where t is the first-neighbor and t_2 is the second-neighbor hopping amplitudes and a is the lattice parameter.

In the two-pole approximation proposed by Roth [13, 14], the Green's function matrix is $\mathbf{G}(\omega) = \mathbf{N}(\omega\mathbf{N} - \mathbf{E})^{-1}\mathbf{N}$ in which \mathbf{N} and \mathbf{E} are the normalization and the energy matrices, respectively [14].

Following the formalism discussed in reference [15], the energy $E = \frac{\langle H \rangle}{N}$ can be written as (N

being the number of sites of the system):

$$E = \frac{i}{2N} \lim_{\delta \rightarrow 0^+} \sum_{\vec{k}, \sigma} \int_{-\infty}^{\infty} f(\omega) (\omega + \mu + \varepsilon_{\vec{k}}) \times [G_{\vec{k}, \sigma}(\omega + i\delta) - G_{\vec{k}, \sigma}(\omega - i\delta)] d\omega \quad (3)$$

where $f(\omega)$ is the Fermi function and the Green's function is

$$G_{\vec{k}, \sigma}(\omega) = \frac{Z_{1,\sigma}(\vec{k})}{\omega - \omega_{1,\sigma\vec{k}}} + \frac{Z_{2,\sigma}(\vec{k})}{\omega - \omega_{2,\sigma\vec{k}}} \quad (4)$$

with

$$Z_{i,\sigma}(\vec{k}) = \frac{1}{2} - (-1)^i \left[\frac{U(1 - 2n_{-\sigma}) - \varepsilon_{\vec{k}} + W_{\vec{k}, \sigma}}{2X_{\vec{k}, \sigma}} \right] \quad (5)$$

and the renormalized bands

$$\omega_{i,\sigma\vec{k}} = \frac{U + \varepsilon_{\vec{k}} + W_{\vec{k}, \sigma} - 2\mu}{2} + (-1)^i \left(\frac{X_{\vec{k}, \sigma}}{2} \right) \quad (6)$$

where $X_{\vec{k}, \sigma} = \sqrt{(U - \varepsilon_{\vec{k}} + W_{\vec{k}, \sigma})^2 + 4n_{-\sigma}U(\varepsilon_{\vec{k}} - W_{\vec{k}, \sigma})}$.

In the grand canonical ensemble, the energy is a function of the chemical potential $E \equiv E(\mu(T))$, where μ changes with the temperature. Therefore, the calculation of $C(T)$ defined as $C(T) = \frac{\partial E}{\partial T}$, must be performed keeping $\langle n \rangle$ constant in the $T - \mu$ plane [8]. Combining equations (3), (4) and $C(T) = \frac{\partial E}{\partial T}$ we get $C(T) = \int_{-\infty}^{\infty} F(\omega) d\omega$ where

$$F(\omega) = f'(\omega)g(\omega) \quad (7)$$

in which $f'(\omega) = \frac{1}{\omega} \frac{\partial f(\omega)}{\partial T}$ and $f(\omega)$ is the Fermi function. The function $g(\omega)$ is defined as:

$$g(\omega) = \frac{1}{2N} \sum_{i=1}^2 \sum_{\vec{k}, \sigma} \tilde{Z}_{i,\sigma}(\vec{k}) \delta(\omega - \omega_{i,\sigma\vec{k}}) \quad (8)$$

where

$$\tilde{Z}_{i,\sigma}(\vec{k}) = (\omega_{i,\sigma\vec{k}} + \mu + \varepsilon_{\vec{k}}) \omega_{i,\sigma\vec{k}} Z_{i,\sigma}(\vec{k}). \quad (9)$$

The band shift $W_{\vec{k}\sigma}$ introduced in equation (6), is: $W_{\vec{k}\sigma} = \frac{1}{n_{\sigma}(1-n_{\sigma})} \frac{1}{N} \sum_{\vec{q}} \epsilon(\vec{k}-\vec{q}) F_{\sigma}(\vec{q})$, where $\epsilon(\vec{k}-\vec{q}) = \sum_{\langle\langle i=0 \rangle\rangle j \neq 0} t_{0j} e^{i(\vec{k}-\vec{q}) \cdot \vec{R}_j}$ and $F_{\sigma}(\vec{q})$ is given in terms of $\langle \vec{S}_j \cdot \vec{S}_i \rangle$, $n_{0j\sigma} = \frac{1}{N} \sum_{\vec{k}} \mathcal{F}_{\omega} G_{\vec{k}\sigma}^{(11)} e^{i\vec{k} \cdot \vec{R}_j}$ and $m_{0j\sigma} = \frac{1}{N} \sum_{\vec{k}} \mathcal{F}_{\omega} G_{\vec{k}\sigma}^{(12)} e^{i\vec{k} \cdot \vec{R}_j}$, where $\mathcal{F}_{\omega} \Gamma(\omega) \equiv$

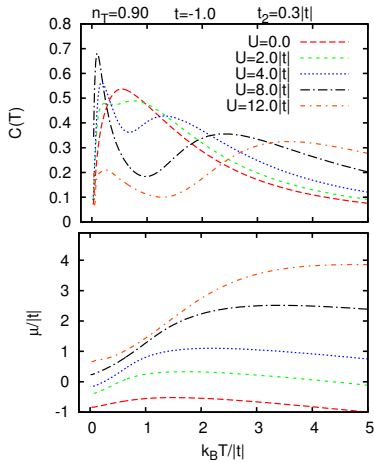


Figure 1: In the upper panel, the specific heat as function of temperature for different values of U . The lower panel shows the chemical potential.

$\frac{1}{2\pi i} \oint d\omega f(\omega) \Gamma(\omega)$, in which $f(\omega)$ is the Fermi function and $\Gamma(\omega)$ a general Green's function. The Green's functions $G_{k\sigma}^{(nm)}$ are obtained as in reference [18]. The spin-spin correlation function is given by:

$$\langle \vec{S}_j \cdot \vec{S}_i \rangle = h_{ij,-\sigma} - \frac{a_{ii\sigma} n_{-\sigma}}{2} - \frac{a_{ij,-\sigma} n_{ij,\sigma} + b_{ij,-\sigma} m_{ij,\sigma}}{1 + b_{ii,-\sigma}}$$

where $h_{ij,-\sigma} = \alpha_\sigma [\bar{n} - (a_{ij,-\sigma} n_{ij,-\sigma} + b_{ij,-\sigma} m_{ij,-\sigma})]$ with $\alpha_\sigma = (1 - b_{ii\sigma}) / [2(1 - b_{ii-\sigma} b_{ii\sigma})]$ and $\bar{n} = n_{-\sigma}^2 (1 - b_{ii-\sigma} b_{ii\sigma})$. Also, $a_{ij,-\sigma} = (n_{ij,-\sigma} - m_{ij,-\sigma}) / (1 - n_\sigma)$ and $b_{ij,-\sigma} = (m_{ij,-\sigma} - n_{ij,-\sigma} n_\sigma) / [n_\sigma (1 - n_\sigma)]$.

3 Numerical results

The upper panel in figure 1 shows the specific heat as a function of temperature for $n_T = 0.90$ and different values of U . For $U = 0.0$, the specific heat presents a peak in the region of $k_B T \approx 0.55|t|$. This peak is known as the Schottky anomaly (see ref. [16] and references therein). However, for $U = 2.0|t|$ the Schottky anomaly starts to split giving rise to a two peak structure. So, for $U = 4.0|t|$ the specific heat shows a peak at low temperature $k_B T \approx 0.2|t|$ and a second peak in $k_B T \approx 1.3|t|$. For $U > 4.0|t|$, the specific heat has a two peak structure, i.e., the high temperature peak persist

even in the strongly correlated limit. The lower panel in figure 1 shows the chemical potential μ as a function of temperature and different Coulomb interactions. The occupation is $n_T = 0.90$, therefore, for $U = 0$ the chemical potential is found below the van Hove singularity. As the temperature increases, μ moves to higher energies in order to keep n_T unchanged. However, when μ reaches the VHS (at $k_B T/|t| \simeq 1.1$), the high density of states in VHS forces the chemical potential back to lower energies to maintain n_T unchanged. When $U \neq 0.0$, a gap opens on the density of states near the VHS and μ increases with temperature until the Fermi function reaches the upper Hubbard band. In this case, for a given temperature, μ can be found within the gap. If temperature increases more, the upper Hubbard band increases its contribution and μ must return to lower energies to maintain n_T unchanged. The behavior of the chemical potential is closely related to the specific heat structure, mainly at low temperatures. We verify that the local minimum in $C(T)$ occurs when μ is found within the gap due to U .

We can understand the two peak structure on $C(T)$ if we analyze the functions $F(\omega)$, $f'(\omega)$ and $g(\omega)$ defined above. The function $g(\omega)$ is shown in the left panel in figure 2 for different Coulomb interactions. The function $g(\omega)$ is directly related to the renormalized density of states, therefore presents a gap due to the Coulomb interaction U . For the model parameters considered in figure 2, in general, $g(\omega)$ is related to the lower Hubbard band if $\omega \lesssim 0.50$ and to the upper Hubbard band if $\omega \gtrsim 0.50$. We verified that at low temperature, the function $f'(\omega)$ is very concentrated on the chemical potential and vanishes quickly for energies that are not close to the chemical potential. Moreover, for $n_T < 1$, the chemical potential is found to be localized in the lower Hubbard band. Then, at low temperatures only the lower Hubbard band contributes to the specific heat and therefore, the low temperature peak on the specific heat is associated to the lower Hubbard band. On the other hand, at high temperatures the function $f'(\omega)$ spreads out, reaches the upper Hubbard band and the specific heat presents a second peak due to the contribution of that band.

Furthermore, as can be verified in figure 1, the position of the second peak in the $k_B T$ axis moves to high temperatures as U increases. This occurs

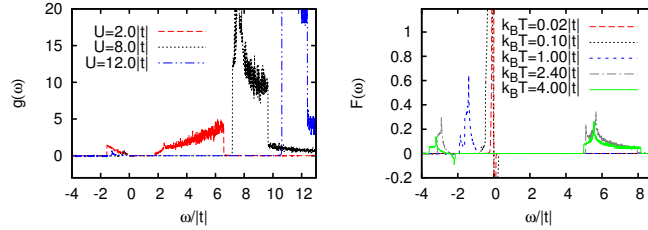


Figure 2: In the left panel the behavior of $g(\omega)$ for $k_B T = 0.03|t|$ and different values of U . The right panel shows the function $F(\omega)$ for $U = 8.0|t|$ and different temperatures. In both panels $n_T = 0.90$, $t = -1.0$ and $t_2 = 0.3|t|$.

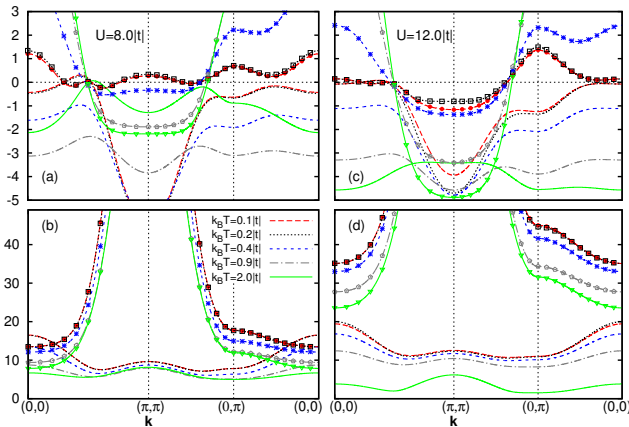


Figure 3: The lines with symbols show the effective spectral weight $\tilde{Z}_{i,\sigma}(\vec{k})$ and the lines with no symbols show the renormalized bands $\omega_{i,\sigma}(\vec{k})$. The upper panels show $\tilde{Z}_{1,\sigma}(\vec{k})$ and $\omega_{1,\sigma}(\vec{k})$ while the lower panels show $\tilde{Z}_{2,\sigma}(\vec{k})$ and $\omega_{2,\sigma}(\vec{k})$. The panels (a) and (b) correspond to $U = 8.0|t|$ and the panels (c) and (d) correspond to $U = 12.0|t|$.

because the upper Hubbard band moves to higher energies as U increases. Consequently, $g(\omega)$ associated to the upper Hubbard band moves also to higher energies and $f'(\omega)$ can reach this region only if $k_B T$ is large enough. Indeed, we verified that the relation between the high temperature peak position and U is $k_B T \approx \frac{U}{3}$. The right panel in figure 2 presents the function $F(\omega)$ (defined in equation (7)) for different temperatures. Due to the relation between $f'(\omega)$ and $F(\omega)$, at low temperatures, $F(\omega)$ is concentrated around the chemical potential μ (localized in $\frac{\omega}{|t|} = 0$). Moreover, $F(\omega)$ presents a negative region near μ that decreases with temperature resulting in an increasing of the specific heat. As a consequence, a peak appears on the specific heat at low temperature. For $k_B T = 1.00|t|$, the negative region in $F(\omega)$ vanishes and the positive

region decreases due to the behavior of $f'(\omega)$. This feature of $F(\omega)$ produces a small value for the specific heat at $k_B T = 1.00|t|$. Increasing the temperature, for instance $k_B T = 2.40|t|$, the intensity of $F(\omega)$ is low for $\frac{\omega}{|t|} < 0$, and a significant region of positive $F(\omega)$ emerges for $\frac{\omega}{|t|} \gtrsim 5.0$. This occurs because at high temperatures $f'(\omega)$ spreads out and reaches the region of $g(\omega)$ associated to the upper Hubbard band. This behavior of $F(\omega)$ enhances again the specific heat giving rise to the high temperature peak. For $k_B T = 4.0|t|$, $F(\omega)$ acts as for $k_B T = 2.40|t|$, however, it decreases the intensity due to the decreasing of the $f'(\omega)$ intensity.

Figure 3 shows the renormalized bands $\omega_{i,\sigma}(\vec{k})$ and the effective spectral weights $\tilde{Z}_{i,\sigma}(\vec{k})$ defined in equations (6) and (9). At low temperatures $\tilde{Z}_{1,\sigma}(\vec{k})$

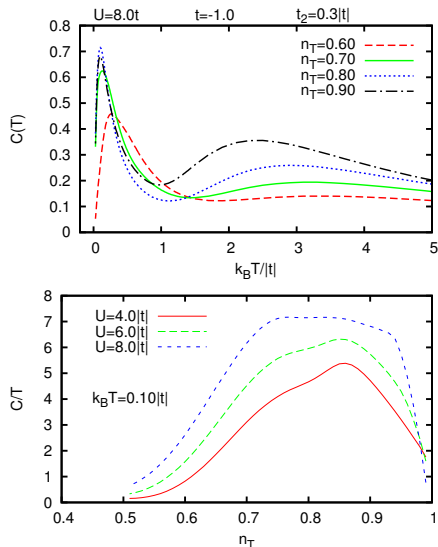


Figure 4: In the upper panel, the specific heat for $U = 8.0|t|$ and different occupations n_T . The lower panel shows the behavior of $\frac{C}{T}$ as a function of the occupation n_T .

is negative only in a small region next to $(\frac{\pi}{2}, \frac{\pi}{2})$. As temperature increases, this negative region enlarges along the direction $(\frac{\pi}{2}, \frac{\pi}{2}) - (0, \pi)$. However, the intensity of $\tilde{Z}_{1,\sigma}(\vec{k})$ is very small. In 3(c), the negative regions of $\tilde{Z}_{1,\sigma}(\vec{k})$ at low temperatures are greater than in 3(a), but its intensity remains small when compared with the intensity of the positive regions.

An important feature observed in $\omega_{1,\sigma\vec{k}}$ is the presence of a pseudogap near $(0, \pi)$. This pseudogap plays an important role relative to the low temperature peak observed on the specific heat. Indeed, the presence of a pseudogap affects strongly $\tilde{Z}_{1,\sigma}(\vec{k})$ which is strongly dependent on $\omega_{1,\sigma\vec{k}}$ (see equation (9)). The opening of the pseudogap in $(0, \pi)$ moves the renormalized band $\omega_{1,\sigma\vec{k}}$ to negative energies. As a consequence, $\tilde{Z}_{1,\sigma}(\vec{k})$ is shifted to the positive region as can be observed, for instance, in figure 3(c), when $k_B T = 0.1|t|$. In (b) and (d), $\tilde{Z}_{2,\sigma}(\vec{k})$ is always positive and increases its intensity with U . The pseudogap emerges when the correlations of antiferromagnetic character associated to the correlation function $\langle \vec{S}_i \cdot \vec{S}_j \rangle$ present in the band shift, become strong sufficiently to push

down the renormalized quasi-particle band $\omega_{1,\sigma\vec{k}}$ in (π, π) [18, 19].

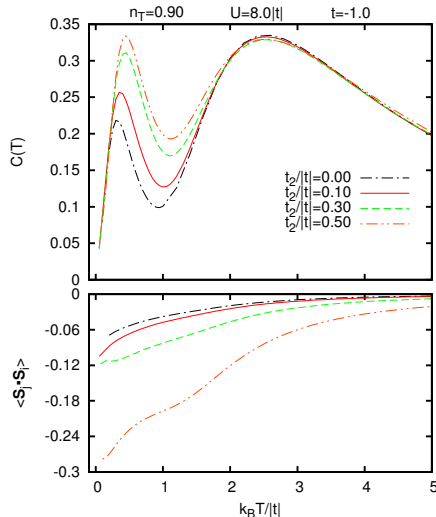


Figure 5: The upper panel shows the specific heat as a function of temperature for different values of $\frac{t_2}{|t|}$. The lower panel shows the spin-spin correlations $\langle \vec{S}_i \cdot \vec{S}_j \rangle$ for the same parameters as in the upper panel.

The upper panel in figure 4 shows the specific heat $C(T)$ as a function of temperature for different occupations. Notice that at low occupations $C(T)$ is characterized by a peak at low temperature. On the other hand, when n_T increases a second peak appears at high temperatures. At low n_T only few electrons reach the upper Hubbard band and therefore the high temperature peak on $C(T)$ is negligible. The behavior of $\frac{C}{T}$ as a function of n_T is shown in the lower panel of figure 4. This results agree qualitatively with those in reference [17]. We verified that for $n_T \gtrsim 0.85$ a pseudogap appears on the anti-nodal points of the renormalized quasi-particle bands (see the lower panel in figure 6). Such pseudogap suppresses the density of states (DOS) on the chemical potential. As the specific heat $C(T)$ is directly related to the DOS, which in turn depends on the renormalized quasi-particle bands, the effects of the pseudogap appearing also on $C(T)$. In the present work, the function $F(\omega)$ defined in equation (7) associates the renormalized quasi-particle band and the specific heat. We verified that the pseudogap suppresses $F(\omega)$,

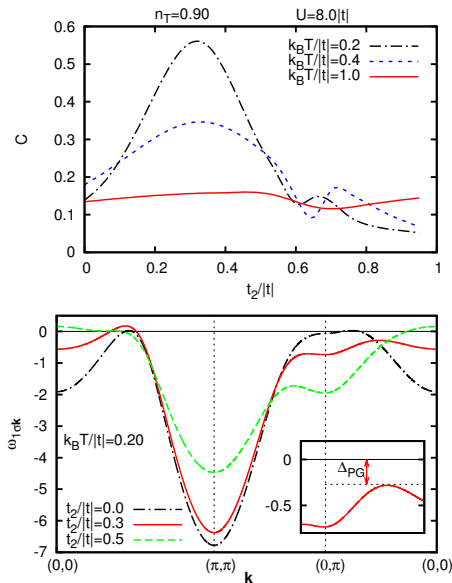


Figure 6: The upper panel shows the specific heat has a function of $\frac{t_2}{|t|}$ and different temperatures. The lower panel shows the renormalized quasi-particle band $\omega_{1\sigma\vec{k}}$ for $k_B T/|t| = 0.20$ and the same parameters as in the upper panel. The inset shows explicitly the pseudogap Δ_{PG} .

below the chemical potential (in $\omega = 0$), resulting in a decreasing in $C(T)$ for $n_T \gtrsim 0.85$. Therefore, it can be concluded that the decreasing of the specific heat above $n_T \simeq 0.85$ in figure 4 is a clear manifestation of the pseudogap.

The effects of the second-nearest-neighbor t_2 on $C(T)$ are shown in the upper panel in figure 5. We observe that the low temperature peak on $C(T)$ is more affected by t_2 than the high temperature peak. The lower panel shows that t_2 enhances significantly the spin-spin correlations $\langle \vec{S}_i \cdot \vec{S}_j \rangle$ which modifies the renormalized quasi-particle bands and consequently the function $F(\omega)$ and therefore, $C(T)$. At low temperature $|\langle \vec{S}_i \cdot \vec{S}_j \rangle|$ is stronger and then its effects on $C(T)$ are more evidenced than at high temperatures. This is the main reason why the low temperature peak on $C(T)$ is more intensively affected by t_2 .

The upper panel in figure 6 shows the specific heat as a function of the second nearest neighbor hopping amplitude $\frac{t_2}{|t|}$ at different temperatures. For $k_B T/|t| = 0.20$ the specific heat presents a maximum for $\frac{t_2}{|t|} \approx 0.30$ and then it decreases until

$\frac{t_2}{|t|} \simeq 0.60$. For $\frac{t_2}{|t|} > 0.60$ the specific heat does not change significantly. The lower panel in figure 6 presents the renormalized quasi-particle band $\omega_{1\sigma\vec{k}}$ for $k_B T/|t| = 0.20$ and three distinct values of $\frac{t_2}{|t|}$. When $\frac{t_2}{|t|} = 0.30$, a pseudogap is observed near the antinodal point $(0, \pi)$. If $\frac{t_2}{|t|}$ increases the pseudogap closes as shown for $\frac{t_2}{|t|} = 0.50$. There is a remarkable coincidence between the maximum on the specific heat and the maximum pseudogap. The analysis of $F(\omega)$ shows that it gives the greater contribution to $C(T)$ when $\frac{t_2}{|t|} = 0.30$. This occurs due to the wide flat region in $\omega_{1\sigma\vec{k}}$ which extends from $(\frac{\pi}{2}, \pi)$ to approximately $(\frac{\pi}{4}, \frac{\pi}{4})$ and gives rise to a very large $F(\omega)$ near the chemical potential. Therefore, even that t_2 opens a pseudogap which suppresses $F(\omega)$ on the chemical potential, it also produces the flat region (near the chemical potential) that overcomes the effect of the pseudogap and increases significantly the specific heat. At high temperatures the pseudogap closes and also the effect of the flat region is suppressed by temperature effects.

4 Conclusions

In summary, the analysis of the two peak structure of $C(T)$ in terms of the renormalized quasi-particle bands allowed us to investigate also a very important feature present in the region of $n_T \gtrsim 0.85$, i. e. the pseudogap region. We observed that above $n_T \approx 0.85$, the specific heat decreases signaling the pseudogap presence. In reference [11], the authors suggest the presence of a pseudogap at half filling of the Hubbard model with Monte Carlo simulation. Here, we confirm the pseudogap existence also out of the half filling.

Acknowledgments

This work was partially supported by the Brazilian agencies CNPq, CAPES, FAPERGS and FAPERJ.

References

- [1] J. Hubbard, Proc. Roy. Soc. **A 276**, 238 (1963).

- [2] J. B. Bednorz and K. A. Müller, Z. Phys. B **64**, 189 (1986).
- [3] T. Timusk and B. Statt, Rep. Prog. Phys. **62**, 61 (1999).
- [4] Patrick A. Lee, Naoto Nagaosa, and Xiao-Gang Wen, Rev. Mod. Phys. **78**, 17 (2006).
- [5] A. Kanigel, *et al.*, Nature Physics **2**, 447 (2006).
- [6] Loram J. W. *et al.*, J. Supercond. **7** 243 (1994); J. W. Loram *et al.*, J. Phys. Chem. Solids **62** 59 (2001).
- [7] T. M. Rice, Kai-Yu Yang, and F. C. Zhang, Rep. Prog. Phys. **75**, 016502 (2012).
- [8] D. Duffy, A. Moreo, Phys. Rev. B **55**, 12918 (1997).
- [9] J. Bonča and P. Prelovšek, Phys. Rev. **B67**, 085103 (2003).
- [10] S. Odashima, A. Avella and F. Mancini, Phys. Rev. **B72**, 205121 (2005).
- [11] T. Paiva *et al.*, Phys. Rev. B **63**, 125116 (2001).
- [12] H. Kusunose, J. Phys. Soc. Jpn. **75**, 054713 (2006).
- [13] L. M. Roth, Phys. Rev. **184**, 451 (1969).
- [14] J. Beenen, D. M. Edwards, Phys. Rev. **B52**, 13636 (1995).
- [15] R. Kishore, S. K. Joshi, J. Phys. C: Solid St. Phys. **4**, 2475 (1971).
- [16] L. Xie, T.S. Su, X.G. Li, Physica **C480**, 14 (2012).
- [17] Tanmoy Das, R. S. Markiewicz and A. Bansil, Phys. Rev. **B81**, 184515 (2010).
- [18] E. J. Calegari, C. O. Lobo, S. G. Magalhaes, C. M. Chaves, A. Troper, Supercond. Sci. Technol. **25**, 025011 (2012).
- [19] M.M. Korshunov and S.G. Ovchinnikov, Eur. Phys. J. **B 57**, 271 (2007).